

## Transport characteristics related to the island divertor geometry of W7-AS

Y. Feng, J. Kisslinger and F. Sardei

*Max-Planck-Institut für Plasmaphysik, Euratom Association, D-85748 Garching, Germany*

### 1. Introduction

Compared to a tokamak divertor, the island divertors proposed for W7-AS and W7-X have the main geometrical features of a small magnetic field line pitch, discontinuous plates and a short radial distance between divertor plates and plasma core. The field shear and the island size are two crucial geometric parameters which govern the plasma transports in the islands. Owing to the low shear and the small island size, the cross-field transports in the island divertor are of greater significance than in tokamak divertors, which gives rise to several specific effects. Understanding the geometry-related effects is essential to improve the divertor performance.

### 2. Geometrical features and diversion properties of the islands

If a rational rotational transform  $\iota = M_{\text{per}}m/n$  ( $M_{\text{per}}$  = number of the toroidal field periods) appears within the configuration, a field component  $B_{mn}$  resonant to that rational  $\iota$  tears the nested flux surfaces apart to form magnetic islands. Although a design principle of low shear stellarators is to avoid low-order resonances within the plasma, a careful choice of  $\iota$  to allow the islands to emerge just at the edge may give rise to a compromise between confinement and exhaust. Depending on the shear  $\iota'$  and the perturbing field  $B_{mn}$ , the radial island size  $r_i$  can be approximated by

$$r_i = 2\sqrt{\frac{R \cdot b_{mn}}{n \cdot \iota'}} \quad (1)$$

where  $R$  is the major radius,  $n$  is the number of the islands and  $b_{mn} = B_{mn}/B_t$ , with  $B_t$  being the toroidal field. The diversion property of the islands arises from the finite shear at the edge. Formally, the rotational transform of the magnetic field line inside the islands can be developed into two parts, i.e.  $\iota = \iota_{m/n} + r_i \iota'$ . The first term represents the  $m/n$  resonance, indicating only the helical rotation of the magnetic islands around the torus. The second is much smaller however more interesting than the first one as it provides an internal poloidal pitch of field lines around the islands, being the basis of an island divertor. It is evident that the island size and the shear are two crucial geometric parameters for the plasma transport in the islands. A comprehensive assessment of their influence on the island divertor performance is beyond the scope of this paper, which, in fact, belongs to the main objects of study throughout the W7-AS divertor program. Instead, we give a rough estimation of their impact on the ratio of parallel to cross-field transports. If we assume that the particle and momentum transports are governed by a parallel classical convection with a sound speed  $C_s$  and a perpendicular anomalous diffusion described by a diffusion coefficient  $D$ , the parallel and perpendicular transport time scales can be roughly estimated as  $\tau_{\parallel} = L_c/C_s$  and  $\tau_{\perp} = 2r_i^2/D$ , respectively. The connection length  $L_c$  (from stagnation point to plate) is given by  $L_c = R\pi/\Delta\iota_i$  with  $\Delta\iota_i = nr_i\iota'/2$  being the internal rotational transform of the magnetic field lines in the islands. Comparison of  $\tau_{\perp}$  with  $\tau_{\parallel}$  yields

$$\frac{\tau_{\perp}}{\tau_{\parallel}} = \frac{n}{R\pi} \frac{C_s}{D} r_i^3 \iota' \quad (2)$$

Let us define  $\tau_{\perp}/\tau_{\parallel} > 1$  as an intuitive criterion for the island divertor without justification. Then equation (2) becomes

$$\frac{r_i^3 t' n}{R} > \pi \frac{D}{C_s}, \quad (3)$$

which relates the geometric parameters to the transport coefficients. Due to the low shear in W7-AS ( about  $3 \times 10^{-3}$  /cm for the 5/9 islands ), the islands must be large enough such that the relation (3) holds. For example, in the case of  $D = 5 \times 10^3$  cm<sup>2</sup>/s and  $C_s = 1 \times 10^7$  cm/s ( corresponding to  $T_e = T_i = 50$  eV ), relation (3) requires that  $r_i$  must be larger than 2.3 cm.

### 3. Transport characteristics

Without additional field perturbations, the 5/9 islands have a  $r_i$  of 3 cm. This implies that the cross-field diffusion plays an important role for the island transports, which leads to several consequences. First of all, cross-field diffusion causes momentum losses of particles flowing to the targets and thus enhances the pressure drop along the separatrix. There are two main momentum loss mechanisms related to the cross-field diffusion. First, particles flow in opposite directions along adjacent island fans to the targets. Momentum loss occurs if the counter-streaming particles exchange their momentum through cross-field diffusion. Secondly, if the particles passing through a flux tube to a plate diffuse into the shadowed region between two plates, they are ‘trapped’ by the plates. Friction between the ‘passing’ and ‘trapped’ particles leads to momentum loss of the ‘passing’ particles.

Quantitative studies of the island transports are carried out by applying the EMC3 code [1]. Pure hydrogen plasmas are assumed. With a fixed power flux of 200 kW through the separatrix, the upstream density  $n_{e,up}$  is varied from  $7 \times 10^{18}$  to  $2 \times 10^{20}$  m<sup>-3</sup>. The diffusion coefficients are related to each other as  $\chi_e = \chi_i = 3D$ . They are kept spatially constant, however scaled with the upstream density roughly as  $1/n_{e,up}$  for  $n_{e,up}$  lower than  $2 \times 10^{19}$  m<sup>-3</sup>. For higher densities,  $D$  is fixed to be 0.25 m<sup>2</sup>/s. The results are summarized in Fig. 1. Shown are the up- and downstream temperature ( $T_{up}$  and  $T_{down}$ ), the downstream density ( $n_{e,down}$ ) as well as the momentum loss factor ( $M_{loss}/p_{down}$ ) as a function of  $n_{e,up}$ . Fig. 1 shows also the results from the two-point model [2] in comparison. In the two-point model the cross-field transports determine the radial width of the parallel flux tube, however, do not directly contribute to the transports from the up- to downstream. Additionally, all the effects mentioned above are not included in the simple model. In contrast, the EMC3 code solves the transport equations in a realistic geometry.

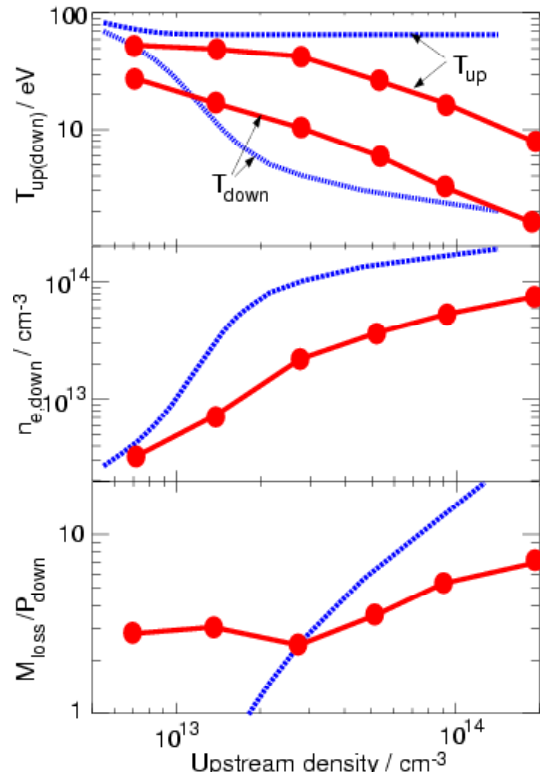


Fig.1 Density scan results from the EMC3 code (solid) and the two-point model (dashed). From top to bottom, up- and downstream temperature, downstream density and the momentum loss factor are plotted against the upstream density.

Two different regimes can be clearly identified from the two-point model, i.e. the linear (low-recycling) regime for  $n_{e,up} < 8 \times 10^{12} \text{ cm}^{-3}$  and the high-recycling regime at  $n_{e,up} > 1 \times 10^{13} \text{ cm}^{-3}$ . The sharp transition from low- to high-recycling is accompanied with a steep rise of the downstream density and a strong drop of the downstream temperature. With further increasing  $n_{e,up}$ , the changes of  $T_{down}$  and  $n_{e,down}$  are moderated by the significant momentum losses from charge-exchange processes. Compared with the two-point model results, the 3D simulations show much smoother changes of  $T_{down}$  and  $n_{e,down}$  with  $n_{e,up}$ . The reason is due to the additional momentum losses specific to the island divertor geometry. The geometry-related momentum losses lead to a parallel pressure drop, even for relative low densities, by a factor of 4-5 instead of 2 and thus prevent  $p_{down}$  from linearly increasing with  $p_{up}$ . Consequently, these momentum losses result in a much smoother transition from low- to high-recycling than that predicted by the two-point model. At high densities ( $n_{e,up} > 3 \times 10^{13} \text{ cm}^{-3}$ ),  $M_{loss}/p_{down}$  increases due to the additional momentum losses resulting from the charge-exchange processes. On the other hand, in this high density range,  $T_{up}$  drops with increasing  $n_{e,up}$ , indicating that the cross-field heat conduction dominates over the parallel one.

At low temperatures the plasma distribution inside the islands becomes strongly inhomogeneous along the island tube. Fig. 2 shows the distributions of ionization source and energy sink due to neutrals as well as density and temperature on a closed island surface over a full toroidal periodicity of nine field periods. The toroidally located bands of ionization sources and the energy losses result from the localization of the recycling neutrals from the discontinuously placed targets and baffles. Temperature drops towards the recycling regions due to the parallel energy fluxes supporting the ionization processes. The density, on the other

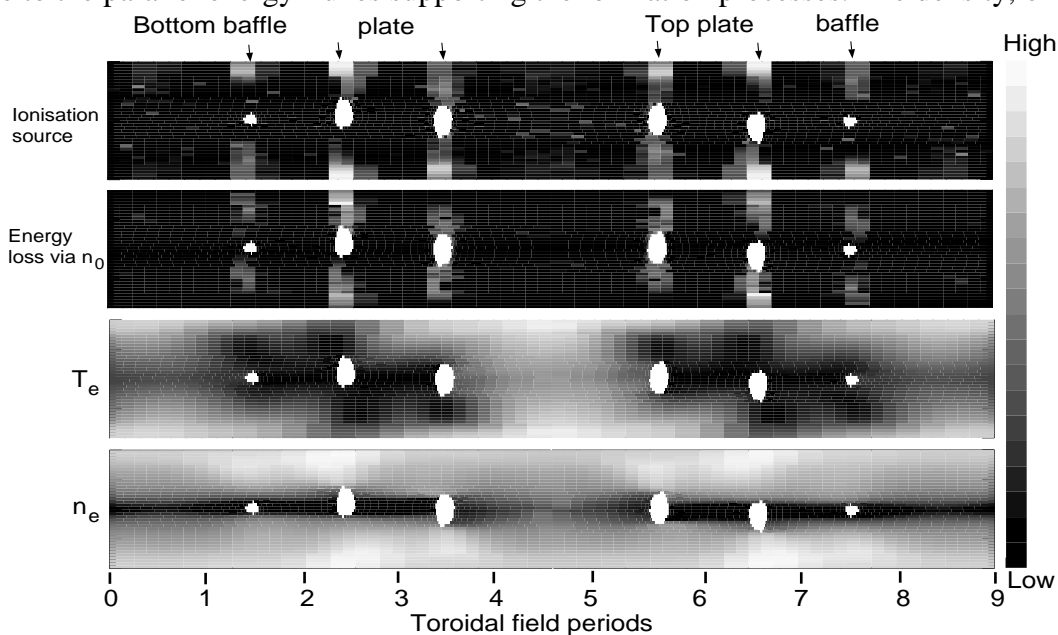


Fig.2 Distributions of ion sources, energy sinks due to neutrals and temperature and density from EMC3 code simulations along an island tube over the full poloidal angle and the full toroidal periodicity of nine field periods. The island tube is cut by each target plate at two adjacent field periods.

hand, shows an opposite phase distribution, in consequence of the momentum balance. The high density at the plates may, to a certain extent, compensate the inefficiency of the ionization process at low temperatures. Owing to the weak dependence of the charge-exchange activity on the temperature, the recycling neutrals can, through charge-exchange, be

deflected poloidally away from the recycling zone and thereby the neutral flux penetrating into the plasma core is reduced.

To reduce the energy flux density to the plates down to a technical limit is an essential task of a divertor. Although the power density on an island divertor plate can in principle be reduced by segmenting and tilting the plate poloidally, this, nevertheless, would restrict the operating configuration range. In addition, associated with the island geometry ( see the lower picture in Fig. 3 ), the island divertor in W7-AS does not benefit from the flux expansion effect as in tokamaks, in which, through this effect, a reduction of the power density on a target plate by a factor of 4 can be achieved [2,3,4]. However, here in the island divertor due to the large ratio of the connection length to the island size, the cross-field heat conduction can effectively broaden the power channel and thus disperse the power density on the targets instead. Fig.3 shows two poloidal power load profiles on a target at  $\phi = 25^\circ$  and  $36^\circ$ , resulting from the EMC3 simulations with  $P = 200$  kW and  $n_{e,up} = 1.5 \times 10^{13} \text{ cm}^{-3}$ . The profiles have a width of about 3 cm, which is by a factor of 5-6 larger than  $2\lambda_T/7$  where  $\lambda_T$  is the radial temperature e-folding distance at the last closed flux surface (LCFS), derived from the perpendicular energy balance.

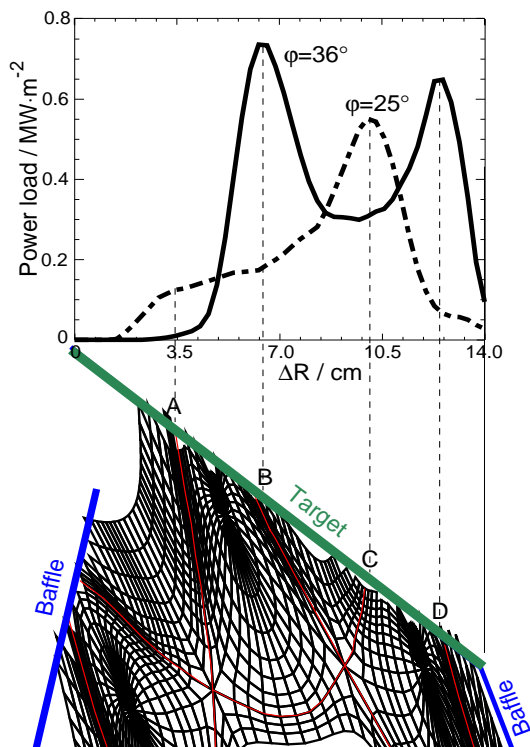


Fig.3 Two poloidal power load profiles on a target at  $\phi = 25^\circ$  and  $36^\circ$ , respectively. The target cuts two islands and the separatrix positions are denoted by A, B, C and D.

#### 4. Summary

In an island divertor, the ratio of the parallel to the perpendicular transport for particle and momentum cubically scales with the island size. For the islands available in W7-AS, the EMC3 code shows that cross-field diffusion causes significant momentum losses of plasma ions on the way to a target, which smoothes the transition from low to high recycling and leads to a parallel pressure drop, under low recycling condition, by a factor of 4-5 instead of 2. In addition, the discontinuous targets give rise to a strong toroidal modulation of the plasma distribution along the island tube, where the density and temperature profiles are phase-shifted to each other. The cross-field heat conduction leads to an effective broadening of the power deposition profiles on the targets. EMC3 simulations show that the power channel onto the W7-AS divertor plates is by a factor of 5-6 broader than that expected from the radial energy balance on the LCFS.

#### References

- [1] Y. Feng, F. Sardei and J. Kisslinger, J. Nucl. Mater. 266-269 (1999) 812-818.
- [2] C. S. Pitcher and P. C. Stangeby, Plasma Phys. Control. Fusion **39** (1997) 779-930.
- [3] G. Janeschitz, Plasma Phys. Control. Fusion **37** (1995) A19.
- [4] G. Janeschitz et al, J. Nucl. Mater. 220-222 (1995) 73.